

# A 55-nm SRAM Chip Scanning Errors Every 125 ns for Event-Wise Soft Error Measurement

Yuibi Gomi, *Student Member, IEEE*, Akira Sato, Waleed Madany, *Member, IEEE*, Kenichi Okada, *Fellow, IEEE*, Satoshi Adachi, Masatoshi Itoh, Masanori Hashimoto, *Senior Member, IEEE*

**Abstract**—We developed a 55 nm CMOS SRAM chip that scans all data every 125 ns and outputs timestamped soft error data via an SPI interface through a FIFO. The proposed system, consisting of the developed chip and particle detectors, enables event-wise soft error measurement and precise identification of SBUs and MCUs, thus resolving misclassifications such as Pseudo- and Distant MCUs that conventional methods cannot distinguish. An 80-MeV proton irradiation experiment at RASiS, Tohoku University verified the system operation. Timestamps between the SRAM chip and the particle detectors were successfully synchronized, accounting for PLL disturbances caused by radiation. Event building was achieved by determining a reset offset with sub-ns resolution, and spatial synchronization was maintained within several tens of micrometers.

**Index Terms**—Soft Errors, Static Random Access Memory (SRAM), Single Event Upset (SEU), Multiple-Cell Upset (MCU), Measurement System

## I. INTRODUCTION

SOFT errors from radiation-induced transient faults challenge modern systems, especially in safety-critical applications such as autonomous driving. Although soft errors in a single device are rare, their occurrence becomes inevitable given the large number of devices.

Soft errors are part of single-event effects (SEEs), and they typically include single-event upsets (SEUs) and single-event transients (SETs). An SEU occurs when radiation strikes an SRAM cell or flip-flop, generating electron-hole pairs that flip a stored bit. Charged particles deposit charge directly, while neutrons deposit charge via the generated secondary ions, potentially causing silent data corruption or detected unrecoverable errors. SEUs appear as either single bit upsets (SBUs) or multiple-cell upsets (MCUs), with MCUs possibly undermining error correction codes (ECC) [1]. In space, protons ionize directly and via secondary ions [2], [3]; on Earth, neutrons dominate, with muons also contributing via nuclear reactions [4]–[7].

Manuscript received \*\* \*\*, 2025; revised \*\* \*\*, 2025.

This work is supported by the Grant-in-Aid for Scientific Research (S) from Japan Society for the Promotion of Science (JSPS) under Grant 24H00073 and JP19H05664.

Yuibi Gomi and Masanori Hashimoto are with the Department of Informatics, Kyoto University, Kyoto 606-8501, Japan (email: hashimoto@i.kyoto-u.ac.jp).

Akira Sato is with the Department of Physics, Osaka University, Toyonaka 560-0043, Japan.

Waleed Madany and Kenichi Okada are with the Department of Electrical and Electronic Engineering, Institute of Science Tokyo, Tokyo 152-8550, Japan.

Satoshi Adachi and Masatoshi Itoh are with the Research Center for Accelerator and Radioisotope Science (RARiS), Tohoku University, Sendai 980-8578, Japan.

The conventional irradiation test writes values into SRAMs, irradiates for a fixed period, and then reads out accumulated bit flips. This approach suffers from issues such as *Pseudo MCU* where independent SEUs are aggregated as a single MCU and *Distant MCU* where bit flips from one particle are misidentified as multiple SEUs. Seifert et al. mitigated the Pseudo MCU issue by continuously reading SRAMs during irradiation to submicron processes and FinFET structures [1], [8]–[11], but Distant MCU remains unaddressed.

This paper proposes a system that simultaneously acquires particle hit timing and location data via a detector and captures SRAM bit flip data. By combining these data streams, our method eliminates Pseudo MCUs and accurately measures SEUs event by event, including Distant MCUs. For this system, we newly designed a 55-nm SRAM chip that scans for errors every 128 clock cycles at a clock frequency of 540 to 1024 MHz and sends error timing and location data to a PC host via FIFO. Proton-beam irradiation experiments verified the chip and system operations.

## II. AN EVENT-WISE SOFT ERROR MEASUREMENT SYSTEM

We have developed an event-wise soft error measurement system, as shown in Fig. 1. Conventional soft error experiments accumulate bit flips over a fixed irradiation period and then map them onto a physical bitmap to classify SEUs into SBUs or MCUs. While efficient, this approach relies solely on location information, leading to the issues described earlier: Pseudo MCU and Distant MCU.

To address these issues, the proposed system integrates a dedicated high-speed SRAM chip, a plastic scintillator, and a Si detector. When a particle strikes the system, the scintillator and the Si detector detect its time and position while the SRAM chip records bit flip locations and timestamps. These four data samples are collectively tracked to identify the particle responsible for each bit flip and group all bit flips caused by the same particle. This approach establishes precise temporal and spatial correlations between bit flips and radiation events, eliminating misclassifications such as Pseudo and Distant MCUs. The key challenges are designing the dedicated SRAM chip and ensuring detector–DUT time synchronization, which are detailed in the following subsections.

### A. Chip Design

A key design specification is the scan interval, which sets the temporal resolution of SEU events based on the SRAM

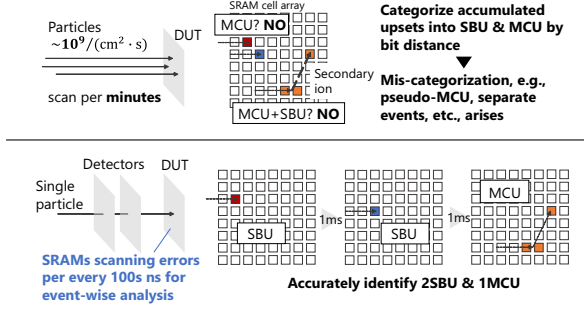


Fig. 1. Conventional (upper) and proposed (lower) methods in radiation testing experiments. The proposed method enables more accurate identification of SBU and MCU events than the traditional upset accumulation.

word count and clock frequency. Thus, an SRAM with fewer words and a higher-frequency PLL are preferable.

Figs. 2 and 3 show a chip block diagram and timing chart, highlighting the rapid error-checking process and secure transfer of error timing and location to the FIFO. The chip contains 36 SRAM macros, each with a one-port, 72-bit, 128-word SRAM, a data pattern generator, and an error-checking mechanism. The error checker outputs an ERROR signal and a 72-bit error data signal with 1s indicating bit flip locations, while a global ERR\_ALL signal is generated by OR-ing all ERROR signals. Redundancy measures, including triple modular redundancy and ECC, ensure functionality and protect error data. A photograph of the 55-nm fabricated chip is shown in Fig. 2; the chip measures 3.88 mm<sup>2</sup>, each macro occupies 0.0363 mm<sup>2</sup>, and the macros cover 33.7% of the core area.

When ERR\_ALL is high, the finite state machine (FSM) transfers error data to the FIFO and clears errors to resume scanning. For instance, if an error occurs at address 0 (as shown in Fig. 3), FIFO\_WDATA, comprising error data, address, timestamp, and macro number, is assembled using a priority encoder and a 36-bit counter, then stored via FIFO\_WE. The FSM also controls the address generator to overwrite the expected value at address 0, while a priority encoder handles simultaneous errors at the same address in different macros. The FIFO supports asynchronous SPI reading, and if no error is detected, the address increments each cycle, ensuring that all 128 words are checked in 128 cycles.

The PLL, implemented with standard cells as in [12], generates a 540 MHz to 1024 MHz clock at 0.9 V to drive the system. Therefore, all cells can be checked within 125 ns at 1024 MHz operation and 237 ns at 540 MHz. This clock is divided by 32 and output as PLLOUT, which is monitored to verify lock status and assist in timestamp retrieval.

For maximum particle flux, all SRAM contents must be read before the next particle arrives. At 540 MHz, if particles arrive at intervals longer than 237 ns, a beam rate of up to 4.21 MHz per macro is feasible, corresponding to  $6.88 \times 10^{10}$  /cm<sup>2</sup>/s. Although random arrival times suggest a lower flux, discarding hits with intervals less than 237 ns avoids drastic flux reduction, demonstrating the system's practicality.

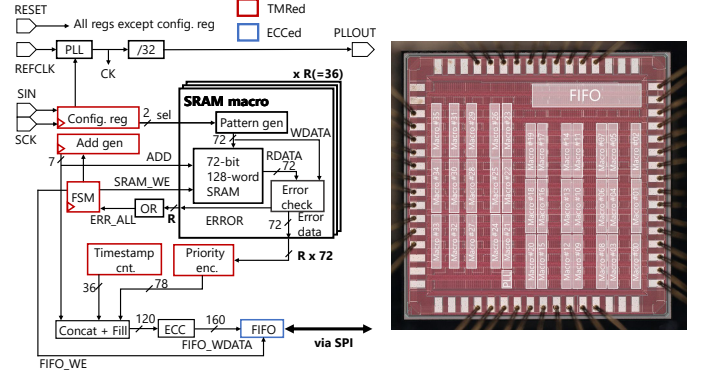


Fig. 2. A block diagram and a photograph of the designed chip.

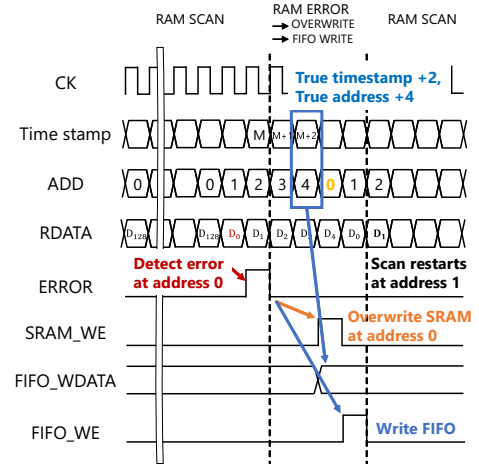


Fig. 3. Timing chart of the designed chip.

### B. Timing Synchronization

It is imperative to correlate soft error data timestamps, which are sourced from the SRAM, PLL, and FIFO in the chip, with the detector data. To accurately reproduce individual events, system-wide timing synchronization is essential. Considering that these physical phenomena occur at the nanosecond scale, synchronization must be performed at the same level. For this, we feed the same reference clock signal to both the detectors and the DUT and initiate their resets using the same reset signal. However, still two problems are to be solved as shown in Fig. 4.

The first problem is that the timestamps of the soft errors will be out of synchronization with the entire system when the PLL in the DUT is affected by radiation. For resolving this issue and synchronizing the timing, PLLOUT, an external output signal obtained by dividing the PLL clock by 32, and the 50 MHz REFCLK are tracked by FPGA counters, with values retrieved every 40 ms via serial communication. When the PLL is locked, actual time is directly derived from their proportional relationship. If unlocked, linear interpolation (LERP) estimates the actual time (Fig. 5).

The second problem is that the system-wide reset signal does not reach every device at the same time. This inherent

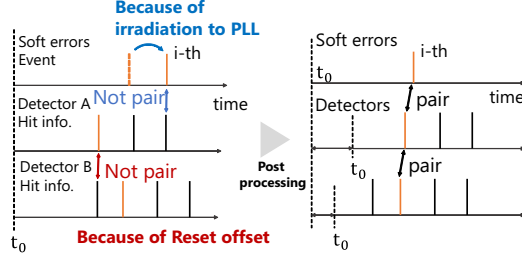


Fig. 4. Pairing of soft errors and hit information from detectors through post-processing. Discrepancies arise due to radiation exposure of the PLL, which generates the internal clock, and the reset offset in the measurement system.

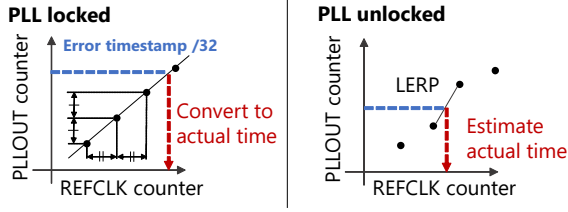


Fig. 5. Methods for obtaining actual time during PLL locked and unlocked states.

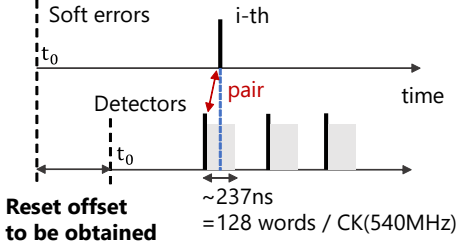


Fig. 6. Synchronization of soft errors and detector hits. The reset offset is determined to pair all soft errors and detector hit information. For a 128-word SRAM and a 540 MHz clock, the detection-to-identification time is within 237 ns.

time lag necessitates determining a reset offset during post-processing. To synchronize detector and soft error events, the reset offset is established as follows: With a 540 MHz clock, time discrepancies of up to 237 ns can arise between error and detector events, as shown in Fig. 6. By applying the reset offset, detector events occurring within this window are identified and paired with their corresponding error events. Among the candidate offsets that enable complete event pairing, the one closest to the average time margin is selected. Here, the average time margin is defined as the expected average discrepancy across all event pairs. For example, at 540 MHz operation, since the time discrepancy between soft error and detector timestamps can be as large as 237 ns and is uniformly distributed, the expected average time discrepancy is 118.5 ns.

### III. EXPERIMENTS FOR SYSTEM VALIDATION

#### A. Setup

Fig. 7 presents the experimental setup at the research center for accelerator and radioisotope science (RARiS), Tohoku University. An 80-MeV proton beam was used for irradiation.

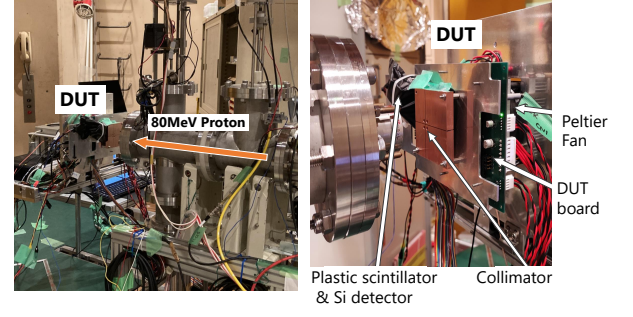


Fig. 7. Irradiation experiment setup at Tohoku University RARiS.

The irradiated system includes a collimator with four holes for four chips, a plastic scintillator with 2 ns resolution, a Si detector with 55  $\mu\text{m}$  resolution, the DUT board, a Peltier cooler, and a fan. Although the board housed 24 chips, only four were activated, with one operating the PLL for analysis. Each 55-nm CMOS chip contained 0.332 Mbit SRAM. Before irradiation, all SRAM cells were initialized to 0, and the supply voltage was set to 0.9 V. When the chip operated above 500 MHz, its current draw exceeded 1 A, causing the temperature to rise above 80  $^{\circ}\text{C}$  and potentially affecting PLL locking. To maintain stable operation, a Peltier cooler, which kept the temperature at 20  $^{\circ}\text{C}$ , was attached to the back side of the DUT board.

#### B. Results and Discussion

By monitoring the PLLOUT signal with an FPGA, we successfully measured and corrected the timestamps. Fig. 8 shows the occurrence frequency and cumulative distribution of the measured PLL output frequency. The PLL output frequency was obtained by multiplying the frequency of the divided PLLOUT signal with 32. While 540.004 MHz accounted for approximately 54% of the measurements, there were instances where the PLL output frequency deviated from this value. The maximum observed frequency was 540.1496 MHz, corresponding to an error of 0.027%, which might be acceptable for typical operations. However, in this experiment, time synchronization at the nanosecond scale is required, making even a 1 Hz deviation significant. To address this, we utilized the post-processing method illustrated in Fig. 5 to calculate the actual time and achieve synchronization with the detector's timing.

Subsequently, using the post-processing method shown in Fig. 6, we determined the reset offset that pairs all soft error events with the detector hit events, where six soft error events were measured in this test run. Initially, the reset offset was varied in 1-ns increments to identify the range of reset offset that successfully paired all soft error events with detector hit events. In the identified range of reset offset, we determined a single reset offset value by calculating the margins between the timestamps of all soft error and detector hit events, and averaging these margins. The results are shown in Fig. 9. In this experiment, the margin is within 237 ns, and the ideal

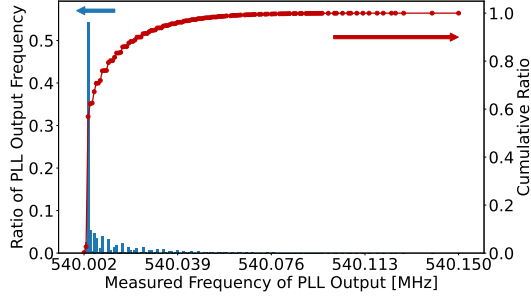


Fig. 8. The occurrence frequency and cumulative ratio of the PLL output observed at the PLLOUT signal. The PLL output is obtained by multiplying the frequency of the divided PLLOUT signal.

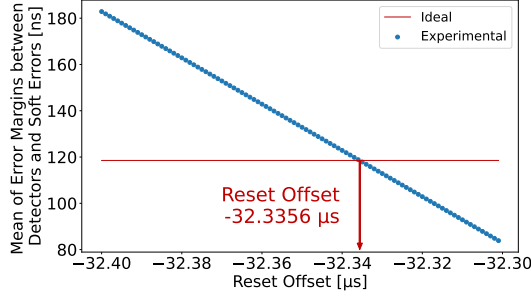


Fig. 9. The mean of the margins between soft errors and detector hits as a function of the reset offset. The reset offset at which the mean margin matches the ideal value is defined as the true reset offset in this experiments.

average value for all margins is 118.5 ns, because the time it takes for a particle to pass through the detector and cause an error, and for the error to be detected, is equally probable for all errors. Based on this analysis, the reset offset of -32.3556  $\mu$ s was identified as the unique reset offset for this experiment.

We listed the coordinate differences for the measured six events in the inset table of Figure 10:  $\Delta x$  and  $\Delta y$  denote the differences in the WL and BL directions, respectively, and  $d$  is the Euclidean distance between the bit flip cell location and the corresponding hit position on the Si detector. The mean of these six distances is 66  $\mu$ m. To validate this result, we built a 3D model of our setup in the particle and heavy ion transport code system (PHITS) [13] better to have a reference and performed Monte Carlo simulations with  $2 \times 10^9$  trials. We then sampled six proton- and secondary-ion-induced SEU events, computed their coordinate differences, and averaged them over  $10^4$  repetitions, with the results shown in Figure 10. The experimentally measured offset was found to be consistent with the simulation.

#### IV. CONCLUSION

This paper proposes an event-wise soft-error measurement system that integrates particle detectors with a newly developed SRAM chip capable of scanning all data in 128 cycles at a clock frequency of 540 to 1024 MHz. An 80-MeV proton irradiation experiment verified that the system can perform sub-ns timing synchronization and event building even while the PLL is unlocked due to radiation. Event building was achieved by determining a reset offset of -32.3556  $\mu$ s to align

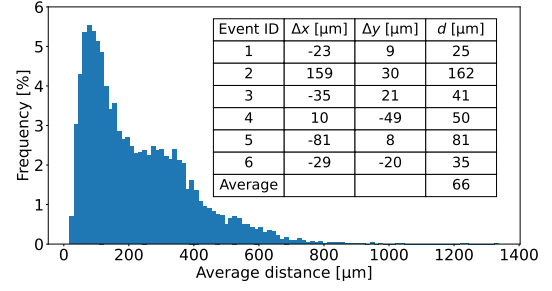


Fig. 10. Histogram of the average distance between the particle hit position on the Si detector and the bit flip cell location, obtained from a PHITS-based Monte Carlo simulation. The inset table gives the measured six events, where  $\Delta x$  and  $\Delta y$  are the coordinate differences in the WL and BL directions, respectively, and  $d = \sqrt{\Delta x^2 + \Delta y^2}$  [ $\mu$ m]. The mean of these distances is 66  $\mu$ m.

soft error and detector hit events, while spatial synchronization was maintained within a few tens of micrometers.

#### ACKNOWLEDGEMENTS

The authors thank Mr. Takahiro Nakayama of Osaka University for his preliminary chip design and analysis.

#### REFERENCES

- [1] J. Maiz *et al.*, "Characterization of multi-bit soft error events in advanced SRAMs," in *IEEE International Electron Devices Meeting*, Dec. 2003, pp. 21.4.1–21.4.4.
- [2] K. P. Rodbell *et al.*, "Low-energy proton-induced single-event-upsets in 65 nm node, silicon-on-insulator, latches and memory cells," *IEEE Transactions on Nuclear Science*, vol. 54, no. 6, pp. 2474–2479, Dec. 2007.
- [3] R. Reed *et al.*, "Heavy ion and proton-induced single event multiple upset," *IEEE Transactions on Nuclear Science*, vol. 44, no. 6, pp. 2224–2229, Dec. 1997.
- [4] B. D. Sierawski *et al.*, "Muon-induced single event upsets in deep-submicron technology," *IEEE Transactions on Nuclear Science*, vol. 57, no. 6, pp. 3273–3278, Dec. 2010.
- [5] S. Manabe *et al.*, "Estimation of muon-induced SEU rates for 65-nm bulk and UTBB-SOI SRAMs," *IEEE Transactions on Nuclear Science*, vol. 66, no. 7, pp. 1398–1403, Jul. 2019.
- [6] Y. Gomi *et al.*, "Muon-induced SEU analysis and simulation for different cell types in 12-nm FinFET SRAMs, and 28-nm planar SRAMs and register files," *IEEE Transactions on Nuclear Science*, 2025, in press.
- [7] D. Measday, "The nuclear physics of muon capture," *Physics Reports*, vol. 354, no. 4, pp. 243–409, Nov. 2001.
- [8] N. Seifert *et al.*, "Multi-cell upset probabilities of 45nm high-k+ metal gate SRAM devices in terrestrial and space environments," in *IEEE International Reliability Physics Symposium*, Apr. 2008, pp. 181–186.
- [9] —, "Radiation-induced soft error rates of advanced CMOS bulk devices," in *IEEE International Reliability Physics Symposium Proceedings*, Mar. 2006, pp. 217–225.
- [10] —, "Soft error susceptibilities of 22 nm tri-gate devices," *IEEE Transactions on Nuclear Science*, vol. 59, no. 6, pp. 2666–2673, Dec. 2012.
- [11] —, "Soft error rate improvements in 14-nm technology featuring second-generation 3D tri-gate transistors," *IEEE Transactions on Nuclear Science*, vol. 62, no. 6, pp. 2570–2577, Dec. 2015.
- [12] B. Liu *et al.*, "A fully synthesizable fractional-N MDLL with zero-order interpolation-based DTC nonlinearity calibration and two-step hybrid phase offset calibration," *IEEE Transactions on Circuits and Systems I: Regular Papers*, vol. 68, no. 2, pp. 603–616, Feb. 2021.
- [13] T. Sato *et al.*, "Recent improvements of the particle and heavy ion transport code system – phits version 3.33," *Journal of Nuclear Science and Technology*, vol. 61, no. 1, pp. 127–135, Oct. 2023.